

Resonance Tunneling in Concentric Quantum Rings

J. Nimmo

North Carolina Central University, Durham, NC, USA, jnimmo@nccu.edu

ABSTRACT

In the present work, the phenomenon known as resonance tunneling due to the presents of a magnetic field perpendicular to the surface of double concentric rings (DCQR) is presented. It has shown that in the weakly coupled DCQR, that has been placed in transverse magnetic field, the electron spatial transition between the rings can occur due to electron level anti-crossing. Resonance tunneling in nano-structures has been of great interest. The ratio of these currents was determined, and the resonance energy and corresponding magnetic field strength were calculated. It will be shown that there are two types current peak: one is associate with anti-crossing and the other is true current resonance. Such results will be useful in cryptography, optics, and quantum computing.

Keywords: tunneling, resonance, quantum rings

1 INTRODUCTION

It has shown that in the weakly coupled DCQR, that has been placed in transverse magnetic field, the electron spatial transition between the rings can occur due to electron level anti-crossing (to avoid energy degeneracy) [1]. In general, there has been an interest in studying the effect of an applied magnetic field perpendicular to quantum rings (QR) [1] - [8]. Double concentric quantum rings (DCQRs) are of interest [1], and [6] – [8] it regards to the study of quantum tunneling because of their rotational symmetry. Resonance tunneling in nano-structures has been of great interest see for example [9] – [11]. In the current work, simulations were conducted using DCQRs composed of GaAs in an $\text{Al}_{0.70}\text{Ga}_{0.30}\text{As}$ substrate thus eliminating the need to consider the effects of stain on the system. For this work the orbital quantum number l was kept at one during all the simulations while varying the transverse magnetic strength from zero to 1.0 T. To measure the level of the tunneling between the rings, the flux through each ring was calculated. In turn the ratio of these fluxes was determine in situation of spontaneous tunneling (i.e. zero magnetic field) as illustrated in figure 1. As seen in this figure, there is one major peek at the 39th energy level which corresponds to a high level of tunneling for zero magnetic field; whereas, the ground there is very little tunneling between the rings. Thus, the focus of the present research was comparison of the tunneling levels of these two energy states (1st and the 39th). In the next section the

details of the calculations and the considerations that were employed are discussed.

2 MODEL

For this research all simulations and sequential calculations were done using a single electron and a single subband approach. When one applies a magnetic field in the z direction ($\mathbf{B} = B\hat{z}$) the Schrödinger equation in cylindrical coordinates can be written as

$$\begin{aligned} & -\frac{\hbar^2}{2} \left(\frac{\partial}{\partial \rho} \left(\frac{1}{m^*} \frac{\partial \Phi_{n,l}}{\partial \rho} \right) + \frac{1}{m^* \rho} \frac{\partial \Phi_{n,l}}{\partial \rho} - \frac{l^2}{m^* \rho^2} \Phi_{n,l} \right) \\ & + \frac{\hbar l \omega_c}{2} \Phi_{n,l} + \frac{m^* \omega_c^2 \rho^2}{8} \Phi_{n,l} + [V_c(\rho, z) - E] \Phi_{n,l} \\ & - \frac{\hbar^2}{2m^*} \frac{\partial^2 \Phi_{n,l}}{\partial z^2} = 0. \end{aligned} \quad (1)$$

Angular coordinates were separated by using

$$\Psi_{n,l}(\rho, z, \phi) = \Phi_{n,l}(\rho, z) e^{il\phi}. \quad (2)$$

Here $n = 1, 2, 3, \dots$ are radial and $l = \pm 0, \pm 1, \pm 2, \dots$ are orbital quantum numbers. $\omega_c = |e|B/m^*$ is the cyclotron frequency. First magnetic field term in (1) is orbital Zeeman term, the second - so called diamagnetic term. The electron spin Zeeman effect has been ignored here since it is small. The double concentric quantum rings were modeled as composed of GaAs in an $\text{Al}_{0.70}\text{Ga}_{0.30}\text{As}$ substrate. The values $m^* = 0.067m_0$ and $0.093m_0$ were used for the bulk values of the effective masses for the DCQR and substrate respectively. The contribution of strain was ignored in this paper because the lattice mismatch between the rings and the substrate is small. The confinement potential $V_c(\mathbf{r})$ was zero in the rings and 0.262 eV in the substrate.

Comsol was used to determine the energy levels for varying magnetic field strengths. The flux through in each ring using

$$S = -2 \frac{\hbar}{m^*} \iint \psi^* \frac{\partial \psi}{\partial r} r \, dr dz. \quad (3)$$

The integration in equation (3) was done over the surface of each ring while normalizing the wavefunction for the individual wavefunction. The ratio (corresponding to each energy) of the average flux through the sending ring to that of the receptive ring as show below:

$$T = \frac{S_{trans}}{S_{inc}} \quad (4)$$

The term S_{inc} is the flux through the sending ring; whereas, S_{trans} corresponds to the flux through the receptor ring. In a similar fashion the R for each energy level was also calculated. To ensure results were consistent with tunneling theory, the sum of T and R was equal to one. Finally, the quantity G was determined as follows:

$$G = G_0 \frac{T}{R} \quad (5)$$

The term $G_0 = 2 \frac{e^2}{h}$ is a constant, with e as the electric charge of an electron and h is Plank's constant. Larger values of $\frac{G}{G_0}$ would indicate higher levels of tunneling "between" the rings with a value of one corresponding to a 50% probability of finding the electron in either ring.

3 EFFECT

Each DCQR was model as a hollow cylinder (with hopes of performing analytical calculation at some time in the future) which have rotational symmetry about the z -axis with a height ($H = 9$ nm), width ($W = 72$ nm), with an inner radius ($R_i = 5$ nm), and a separation between the rings ($S = 5$ nm). Such a choice of geometric parameters corresponding to those using in previous literature ensuring geometric symmetry at $B = 0$ and yielding over 40 energy levels. To establish a base line, the value of G was calculated for every energy level at $B = 0$ as shown in Figure 1.

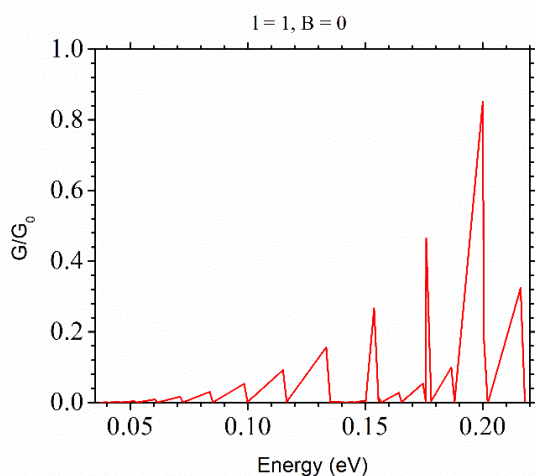
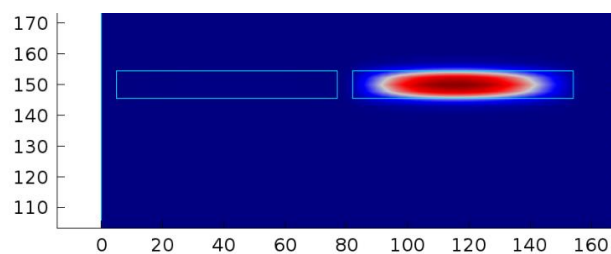
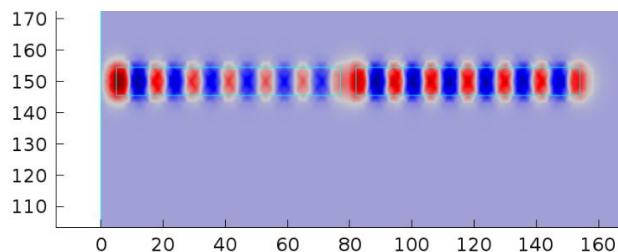


Figure 1. The G values corresponding every energy level (total of 44) at magnetic field strength of $B = 0$ and orbital quantum number $l = 1$.

Figure 1 shows that a peek for $\frac{G}{G_0}$ with $B = 0$ occurs at the 39th energy level with a value of about 0.85 whereas for the ground state its value is near zero ($\sim 10^{-5}$), thus greatly contrasting the spontaneous tunneling activity in the 39th energy and the ground state. To better understand this result one can look one at Figure 2. The top of Figure shows that there is very little tunneling between the rings, thus if an electron is in the outer ring it will trend to stay there. On the other hand, the situation shown on the bottom illustrate a high level of tunneling between the rings. Although there is about 80% chance of the electron being in the outer ring, there is a 11% probability of it being in the inner ring and 9% chance of being in the substrate (tunneling). Figures 1 and 2 b both show that the 39th state exhibits a high level of spontaneous tunneling between the rings as compare to the ground state. This situation would seem to suggestion a situation that is akin to that of normal modes of vibrations in classical mechanics.



a.

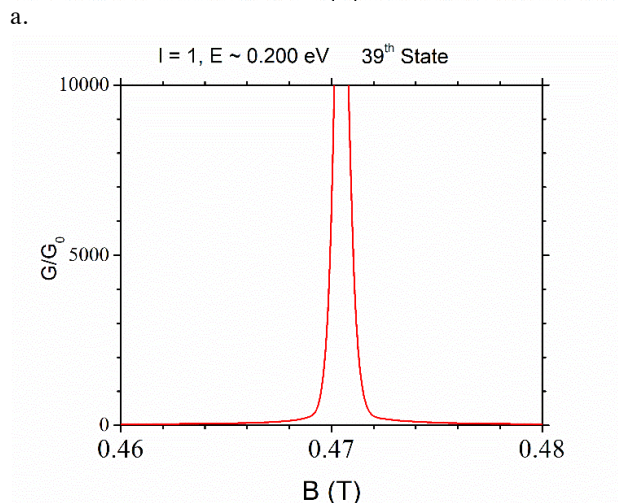
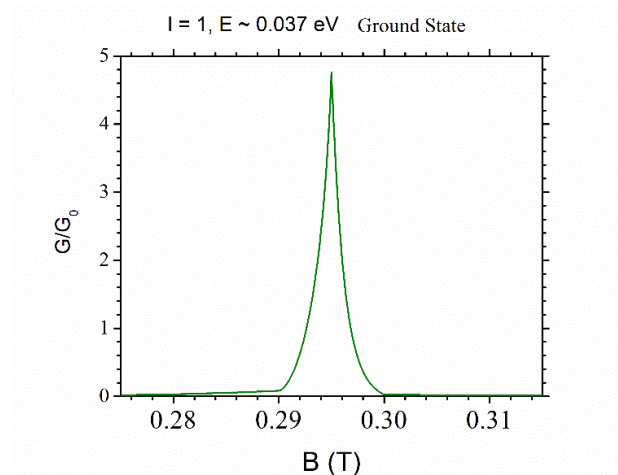
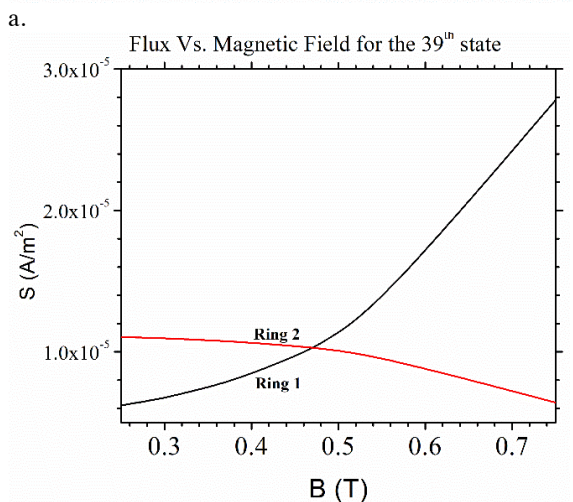
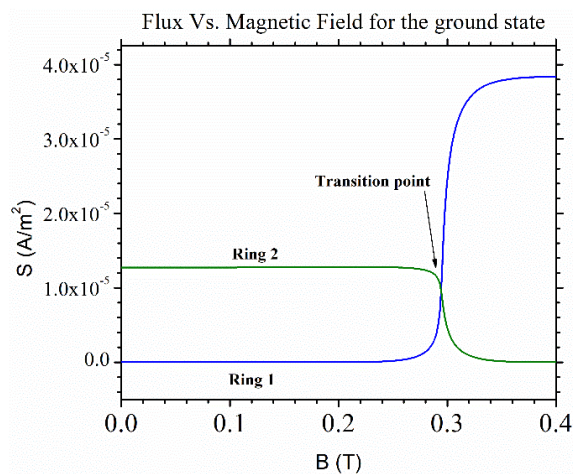


b.

Figure 2. Screen shot from Comsol illustrating a cross-section of the ring superimposing a graph of the wavefunction (ψ) as function of special coordinates (r, z) as measured in nm with $B = 0$ and $l = 1$. The top is for the 1st energy ($E \sim 0.037$ eV) and the bottom is for the 39th energy state ($E \sim 0.20$ eV).

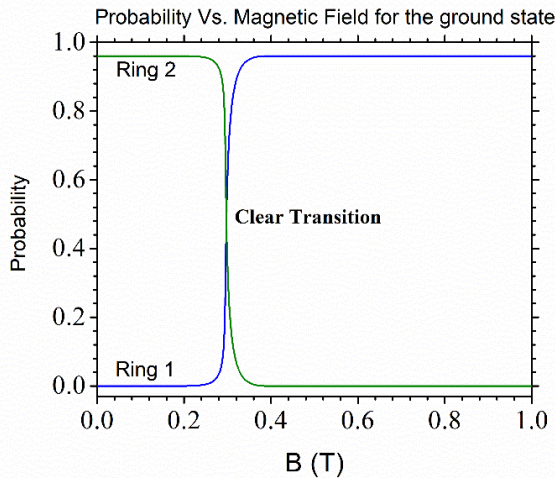
Figure 3 shows that G as a function of applied magnetic field strength (B). Both graphs exhibit a peak for value for G when plotted as a function of the applied magnetic field strength (B); however, the peak for the 39th state is several orders of magnitude larger than that of the ground state. The top part of Figure 4 show that for the lowest energy state, the flux through ring 1 (the inner ring) remains relatively low until the transition point (see [1]) where it dramatically increases and the flux through ring 2 decreases by several orders of magnitude. In sharp contrast, the bottom part of Figure 4 illustrates as magnetic field

strength (B) increases, the flux through ring 1 smoothly and slowly increases increasing, whereas the flux through ring 2 smoothly and slowly decreases. At the magnetic field strength (B) where the two curves cross each other, the peak for G occurs. Figure 5 a show the probability of finding the electron in a ring flips (transition point) about $B = 0.295$ T coincides with the G peak shown in Figure 3 a for the ground state of the electron. The occurrence of the G peak for the ground state corresponding to its transition point for this energy can be explained by anti-crossing of the energy levels in agreement with Filikhin et al. In sharp contrast to Figure 5 a, Figure 5 b illustrates that the peak G for an electron in the 39th energy state before the crossing of the corresponding of its probability curves which trend in opposite directions, but it doesn't show a clear transition point. This sharp contrast in probability curves shown in Figure 5 and the correspondence of the peaks shown in Figure 3 would indicate that there are two different mechanism involved to cause the G peaks.

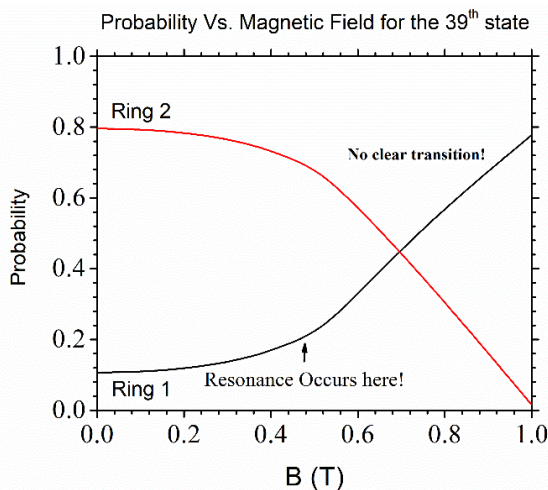


b. Figure 4 Flux through each ring as a function of magnetic field strength (B) corresponding to the ground state on top (a.) compared to the 39th as shown on the bottom. The top part also shows the transition point. The point of intersection of the two curves shown on the bottom corresponds with location of \tilde{G} in Figure 3 b.

b. Figure 3 G as function of magnetic field strength (B) corresponding to the ground state shown on top (a.) compared to the 39th as shown on the bottom (b).



a.



b.

Figure 5 Probability of finding an electron in ring 1 vs. ring 2 as a function of magnetic field strength (B) is shown for the ground state in the top (a.) as compared with the 39th state illustrate on the bottom (b.).

4. CONCLUSION AND FUTURE WORK

A thorough study of resonance tunneling in concentric quantum rings was completed. Throughout this study the orbital angular momentum (l) was kept at one. Tunneling (at $B = 0$) was examined by calculating a quantity G for 44 energy levels as illustrated in Figure 1 showing a peak for the 39th energy level. Figures 1 and 2 set-up a strong case for a situation that is akin to that of normal modes of vibrations in classical mechanics. Although such results are compelling, they are not conclusive; therefore, further study focusing on these results is warranted. Peaks were found for the quantity G for the first and 39th energy levels when G was graph as function of B for these energy levels; however, the G peak

corresponding to the 39th energy level was several orders of magnitude greater than the one for the first energy level.

Figures 3 through 5 illustrate a sharp contrast in the response to an electron tunneling due to magnetic field applied perpendicular to a DCQR system for two different energy levels. Resonance tunneling can occur in a single electron system. A combination of these results as discussed above and the huge difference in the G peaks would suggest two different mechanisms are responsible for these peaks. The peak corresponding to the ground state energy level is due to energy anti-crossing which agrees with the results of Filikhin et al. These results suggest that the mechanism for the peak corresponding to the 39th energy level is akin to that of normal mode vibrations resulting in a true resonance; whereas, the peak for the ground state is a mere blimp in the curves due to the anti-crossing of energy states.

Future research will explore the relationship between the individual rings and the DCQR system to determine the nature of the ring coupling and whether a connection can be made to normal modes of vibrations as lay out in classical mechanics. The effect of a Coulomb interaction in a two-electron system will be examined. Finally, the role of quantum Chaos will be examined.

References

- [1] I. Filikhin, S. Matinyan, J. Nimmo, B. Vlahovic, *Physica E* **43** 1669–1676 (2011).
- [2] J. A. Vinasco et al, *Scientific Reports* **9**, 1427 (2019).
- [3] L. L. Li, D. Moldovan, P. Vasilopoulos, and F. M. Peeters, *Phys. Rev. B* **95** 205426(2017).
- [4] Lafy. F. AL-Badry, *Solid State Communications*, **254**, 15 – 20 (2017).
- [5] H. M. Baghrmryan et al, *Scientific Reports* **8** 6145 (2018).
- [6] T. Mano, et al, *Nano Lett.* **5** 425 (2005).
- [7] B. Szafran and F. M. Peeters, *Phys. Rev. B* **72**, 155316 (2005).
- [8] J. Climente, J. Planelles, M. Barranco, F. Malet, M. Pi *Phys. Rev. B* **73**, 233102 (2006).
- [9] L. L. Chang, L. Esaki, and R. Tsu, *Appl. Phys. Lett.* **24** 593(1974).
- [10] Y. S. Joe, A. M. Satanin, C. S. Kim, *Phys. Scr.* **74**, 259–266 (2006).
- [11] K. Sugiyama, T. Okunishi, M. Muraguchi, K. Takeda, *Phys. Rev. B* **81**, 115309 (2010).